Proc. Natl. Acad. Sci. USA
Vol. 96, pp. 9427–9432, August 1999
Physiology

Chemoreceptor discharges and cytochrome redox changes of the rat carotid body: Role of heme ligands

SUKHAMAY LAHIRI*, WILHELM EHLEBEN†, AND HELMUT ACKER†‡

†Max Planck Institut für Molekulare Physiologie, D-44227 Dortmund, Germany; and *Department of Physiology, University of Pennsylvania School of Medicine, Philadelphia, PA 19104-6085

Communicated by Robert E. Forster, University of Pennsylvania School of Medicine, Philadelphia, PA, June 10, 1999 (received for review December 3, 1998)

ABSTRACT **In superfused *in vitro* rat carotid body, we recorded chemoreceptor discharges and the redox state of cytochromes simultaneously to identify the primary oxygen-sensing protein controlling transmitter release and electrical activity of the carotid sinus nerve. These parameters were tested under the influence of heme ligands such as oxygen, cyanide, 4-(2-aminoethyl)-benzenesulfonyl fluoride, and CO. During stimulation, there was an initial increase in discharge frequency followed by a decline or suppression of activity. Photometric changes lagged and were maintained as nerve activity decreased. Reducing mitochondrial cytochromes by cyanide or prolonged severe hypoxia, suppressed the chemoreceptor discharge. 4-(2-Aminoethyl)-benzenesulfonyl fluoride, a specific inhibitor of the phagocytic cytochrome b_{558}, also silenced the chemoreceptors after an initial excitation. CO increased the chemoreceptor discharge under normoxia, an effect inhibited by light, when the cytochromes were not reduced. When the discharges were depressed by severe hypoxia, exposure to light excited the chemoreceptors and the cytochromes were reduced. The rapidity of the chemosensory responses to light and lack of effect on dopamine release from type I cells led us to hypothesize that carotid body type I cells and the apposed nerve endings use different mechanisms for oxygen sensing: the nerve endings generate action potentials in association with membrane heme proteins whereas cytosolic heme proteins signal the redox state, releasing modulators or transmitters from type I cells.**

It has been hypothesized that the signal cascade leading to PO_2-dependent chemoreception in the carotid body consists of a heme protein-sensing oxygen, which under hypoxia, closes potassium channels with consequent depolarization of type I cells. This closing is followed by an influx of calcium through voltage-dependent calcium channels and liberation of transmitters. The latter generate action potentials in synaptically apposed nerve endings that travel via the carotid sinus nerves to the brainstem to regulate respiration and circulation (1). It has been proposed that the oxygen-sensing heme proteins behave like the mitochondrial cytochrome aa_3, with an unusually low PO_2 affinity (2–4), or like nonphagocytic low-output NAD(P)H oxidase-generating oxygen radicals depending on PO_2 (5, 6).

To understand the nature of the oxygen-sensing heme protein we studied the influence of different heme ligands, such as oxygen, cyanide, 4-(2-aminoethyl)-benzenesulfonyl fluoride (AEBSF), and CO on simultaneous chemoreceptor discharge and the redox state of mitochondrial and nonmitochondrial cytochromes. We used the rat carotid body, superfused *in vitro*, to record simultaneously the sinus nerve electrical activity and optical density changes in the tissues. We will show that the initial chemoreceptor excitation is not coupled to detectable reduction of the cytochromes. Reduction of the respiratory chain by severe hypoxia or cyanide, and inhibition of cytochrome b_{558} by AEBSF (7), depresses the chemoreceptor discharge. CO binds (in a photolabile manner) to a heme protein (similar to cytochrome *a*), leading to excitation of the chemoreceptor discharge under normoxia and inhibition under hypoxia. This heme protein has not been detected by optical density measurements but by action spectrum analyses (4). Because the light effects on CO-bound heme protein are fast, it suggests they are located in the sinus nerve endings.

MATERIALS AND METHODS

Experimental Conditions. Rats (150–200 g) were anesthetized with a mixture of 25% urethane and 4% chloralose (0.45 ml/100 g). The carotid artery bifurcation and carotid body were surgically exposed, and the sinus nerve was cut near its junction with the glossopharyngeal nerve. To clear red cells from the carotid body, the carotid arteries were perfused with oxygenated isotonic salt solution for 10 min after heparinizing the animal with liquemin (1.3 USP-E/g) injected into the jugular vein. Further clearing of red cells from the carotid body vasculature was done by injecting oxygenated isotonic salt solution into the occipital artery. The carotid body and sinus nerve were freed from connective tissue, dissected out from the bifurcation, and placed in chilled, oxygenated isotonic salt solution (containing 128 mM NaCl, 5.6 mM KCl, 27.5 mM glucose, 17 mM Hepes, and 2.1 mM $CaCl_2$).

Light Absorption Photometry. The isolated carotid body and sinus nerve were placed in a superfusion chamber mounted on top of an opaque bench containing small holes of diameters similar to that of the carotid body. The system was mounted on the stage of a light microscope (Olympus) for light absorption measurements as described (9, 10). White light from a halogen bulb (12 V, 100 W) passing through an objective (40×), transilluminated the carotid body for 10 s every minute. Superfusion was done as described (8). Briefly, an isotonic salt solution (128 mM NaCI, 5.6 mM KCI, 27.5 mM glucose, 7 mM Hepes, 10 mM $NaHCO_3$, 2.1 mM $CaCl_2$) was equilibrated with different O_2/CO_2 mixtures to adjust oxygen tensions to various levels at pH about 7.4. Saline flowed through the chamber at 60 ml/min. Temperature was maintained at 36°C.

Transillumination induced absorption changes at different wavelengths, recorded by a photodiode-array spectrophotometer (MCS 210, Zeiss) connected to the third ocular of a trinocular head of the microscope via a light guide. Differential spectra were obtained by first recording in the superfusion medium equilibrated with 28.8% O_2, 4% CO_2, and 67.2% N_2 (aerobic steady state). These spectra automatically were sub-

The publication costs of this article were defrayed in part by page charge payment. This article must therefore be hereby marked "*advertisement*" in accordance with 18 U.S.C. §1734 solely to indicate this fact.

PNAS is available online at www.pnas.org.

Abbreviation: AEBSF, 4-(2-aminoethyl)-benzenesulfonyl fluoride.

‡To whom reprint requests should be addressed at: Max Planck Institut für Molekulare Physiologie, Otto-Hahn-Straβe 11, D-44227 Dortmund, Germany. E-mail: helmut.acker@mpi-dortmund.mpg.de.

tracted from those obtained under reduced conditions, produced by equilibrating the saline with different concentrations of N_2, O_2, CO, or cyanide at constant CO_2 (4%). Adjustments of the gas concentrations were done with two gas mixing pumps (Wösthoff, Bochum, Germany). The differential spectra were evaluated, deconvoluted, and visualized by using the software package TECH PLOT (R. Dittrich, Software für Forschung und Technik, Braunschweig, Germany).

Sinus Nerve Activity. A glass microelectrode (tip diameter 130–160 μm) filled with isotonic salt solution was used to suck in the cut end of the sinus nerve, to record chemoreceptor afferent discharges. The electrode was connected to a differential preamplifier (model DAM-5A, WPI Instruments, Waltham, MA) in turn connected to a window discriminator (model 121, WPI Instruments) used with a rate meter. Counting rates of the action potentials and transillumination time of the carotid body were stored with the aid of a computer program. The action potentials were displayed on an oscilloscope (TDS 210, Tektronix).

RESULTS

Eleven carotid bodies were successfully cleared of red cells to characterize the influence of oxygen, cyanide, and CO on the chemoreceptor discharge and redox changes of different cytochromes. All experiments started with an extended period of severe hypoxia produced by equilibrating the superfusion medium with 96% N_2 and 4% CO_2 for about 4 min. Fig. l*a* gives a typical example. The left side (impuls/sec) shows the time course of the chemoreceptor discharge, responding to hypoxia with a large transient peak and subsequent stabilization at lower discharge levels. After returning to normoxia, the chemoreceptor discharge showed significant depression reaching control levels in about 30 min (data not shown). The time points of spectral analyses and duration of transilluminations are shown by black bars (shutter). The N_2 spectra versus aerobic spectra [wavelength (nm)] clearly show absorption peaks at 550 and 602 nm and a shoulder at 560 nm, with the highest degree of optical density changes at the end of the hypoxic period. Because these spectra are produced by different mitochondrial and nonmitochondrial cytochromes, differential spectra of various isolated cytochromes were used in a deconvolution procedure (9, 10). The purpose was to identify peaks and shoulders and to fit the experimental curve to a superposition curve.

The curves in Fig. 2*a*, marked with different symbols and named according to their origin, correspond to redox differential spectra of isolated mitochondrial cytochrome *c* peaking at 550 nm, cytochrome *b* peaking at 563 nm, and cytochrome aa_3 peaking at 605 nm as described by Chance *et al.* (11). Nonmitochondrial cytochrome *b* peaked at 558 nm, as described by Thelen *et al.* (12) for the phagocytic high-output NADPH oxidase. These cytochromes occur in carotid body tissue (6, 13). The amplitude of the optical density for the spectra of isolated cytochromes was varied for deconvolution to fit as close as possible to the experimental curve (solid line) with a superposition curve (filled circles) representing the sum of the optical densities of the different cytochromes at each wavelength. The experimental curve is a mean curve of the most reduced spectrum with 4-min hypoxia of the 11 carotid bodies. The peaks at 550 nm and 602 nm of the experimental curve are clearly related to isolated cytochromes *c* and aa_3. The peak of isolated cytochrome aa_3 is shifted to 605 nm because of its reduction by cyanide (11). This shift of the peak wavelength between hypoxia- and cyanide-reduced cytochrome aa_3 also was observed in our experiments when the carotid bodies were exposed to cyanide (Fig. 2*c*). The shoulder appears to be produced by cytochromes b_{563} and b_{558}. Deconvolution of the spectrum (shown in Fig. 2*a*) allows one to relate the maxima of the different cytochromes to each other and to

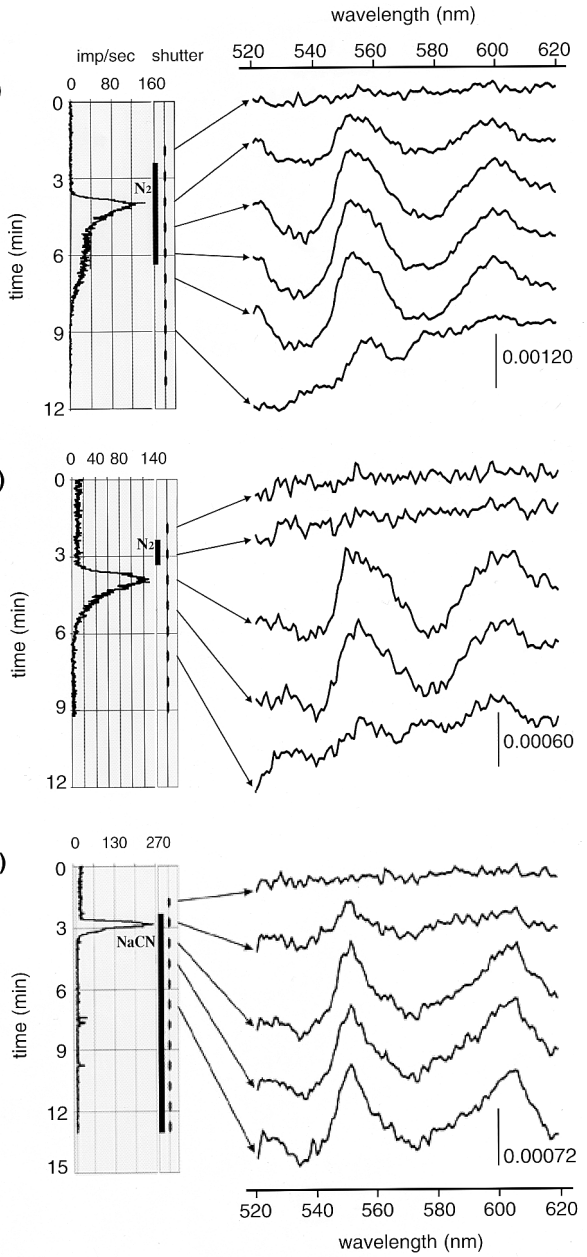

FIG. 1. Simultaneous recordings of chemoreceptor discharges (*Left*, impuls/s) and light absorption spectra (*Right*, wavelength, nm). (*a*) Four-minute hypoxia shown by bar N_2. (*b*) One-minute hypoxia marked by bar N_2. (*c*) Long exposure to 500 μM NaCN marked by bar NaCN. Transillumination periods to record light absorption spectra shown by small bars in shutter.

assess the influence of prolonged hypoxia on this relationship. It suggests a change in the redox state of the different cytochromes. With 4-min hypoxia, cytochromes *c*, b_{558}, b_{563}, and aa_3 are related as 1:0.3:0.77:1.4. The ratios indicate that the degree of reduction by N_2 depends on the oxidation state of the cytochromes under 28.8% O_2. Cytochrome aa_3, normalized to cytochrome *c*, is oxidized to the highest degree as one would expect from the different redox potentials of the respiratory chain cytochromes.

Fig. 1*b* gives an example of exposing the carotid body to a hypoxic period of 1 min. The peak of the nerve discharge is accompanied by optical density changes, which can be easily related to the different cytochromes by deconvolution as shown in Fig. 2*b*, averaging the most reduced spectra of five carotid bodies. Cytochromes *c*, b_{558}, b_{563}, and aa_3 are related as 1:0.4:0.7:1.4.

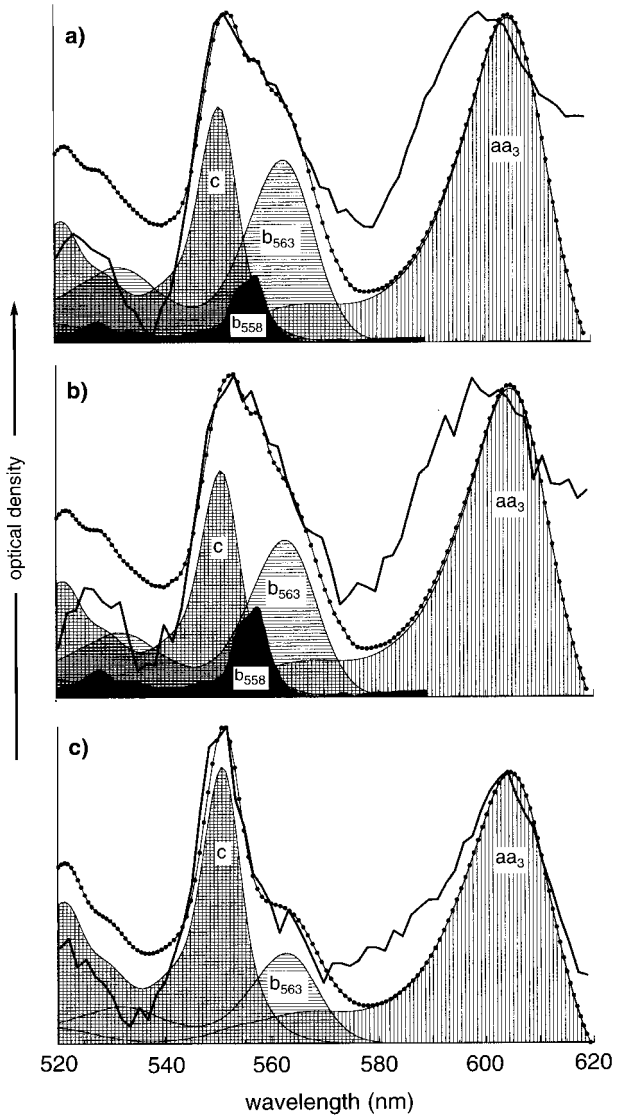

FIG. 2. Deconvolution of light absorption spectra recorded during (*a*) 4-min hypoxia ($n = 11$), (*b*) 1-min hypoxia ($n = 5$), and (*c*) 500 mM NaCN ($n = 6$). Basic redox spectra of isolated cytochrome *c* peaking at 550 nm (*c* crosshatched lines), cytochrome b_{558} (b_{556}, dark shaded), cytochrome b_{563} (b_{563}, parallel line), and cytochrome aa_3 peaking at 605 nm (aa_3, vertical lines). Light absorption changes of spectra of isolated cytochromes are relative values calculated to fit experimental curve (solid line) as close as possible by a superposition curve (●). Experimental curve is mean of most reduced spectra under 4-min hypoxia of 11 carotid bodies, under 1-min hypoxia of five carotid bodies, and under 500 μM NaCN of six carotid bodies, respectively.

Fig. 1*c* shows an example of the relationship between chemoreceptor discharges and redox changes of cytochromes under 500 μm NaCN. After a short peak, the chemoreceptor discharge was eliminated and could not be elicited by stimuli such as hypoxia, CO_2, cyanide, or CO. This suppression is accompanied by significant reduction of the mitochondrial cytochromes as revealed in Fig. 2*c*, by deconvolution of the most reduced spectra of six carotid bodies. Under cyanide, cytochromes *c*, b_{563}, and aa_3 are related as 1:0.33:0.99 without any detectable reduction of cytochrome b_{558}. It should be noted that the spectra obtained under 1-min hypoxia are 1:2.8 and under cyanide a smaller amplitude of spectra was obtained than those resulting from 4-min hypoxia. Despite different patterns of cytochrome absorption and degrees of cytochrome reductions under the three conditions, the chemoreceptor discharges had similar peaks as shown in Fig. 3. The discharge

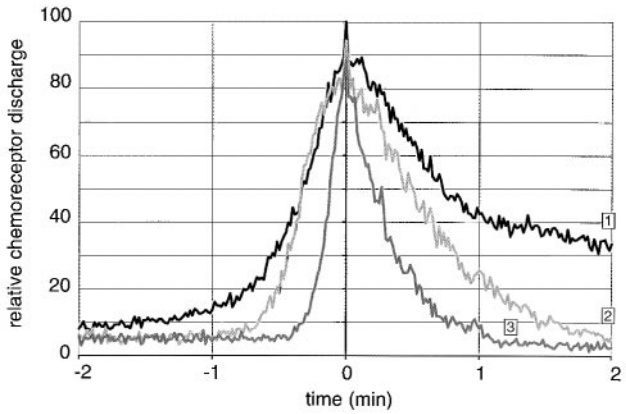

FIG. 3. Chemoreceptor discharge with 1-min hypoxia (marked as 2, $n = 5$) and 500 μM NaCN (marked as 3, $n = 6$) expressed as percentage of peak chemoreceptor activity of 4-min hypoxia (marked as 1, $n = 11$). Peak activity under all stimuli reaches same height. Time (min) to (−) and from (+) the peak. Stimuli started to trigger chemoreceptor activity between 0.5 and 0.9 min.

peak, obtained under prolonged hypoxia (marked as 1), was taken as 100% and compared in each experiment to the chemoreceptor response obtained with 1-min hypoxia (marked as 2) and applications of cyanide (marked as 3). The degree of decline in chemoreceptor discharges was different, in spite of continuous stimulation under prolonged hypoxia and cyanide.

Because deconvolution analyses showed cyanide insensitivity of cytochrome b_{558} but a significant difference in the decline of chemoreceptor discharges, we applied AEBSF (a specific inhibitor of phagocytic cytochrome b_{558}, ref. 7) in four experiments. During superfusion with 2 mM AEBSF, Fig. 4 shows depression of chemoreceptor discharges after an initial excitation. Under these conditions, hypoxia, cyanide, CO_2, and CO were unable to increase the chemoreceptor discharge. Washing out AEBSF produced significant overshoot of the nerve discharge, which returned to control levels in about 30 min (data not shown). Superfusion with the analogue AEBSNH2, in which an amide group replaces the fluoride in AEBSF and is less inhibitory (7), depressed the chemoreceptor discharge without the initial excitation followed by inhibition induced by

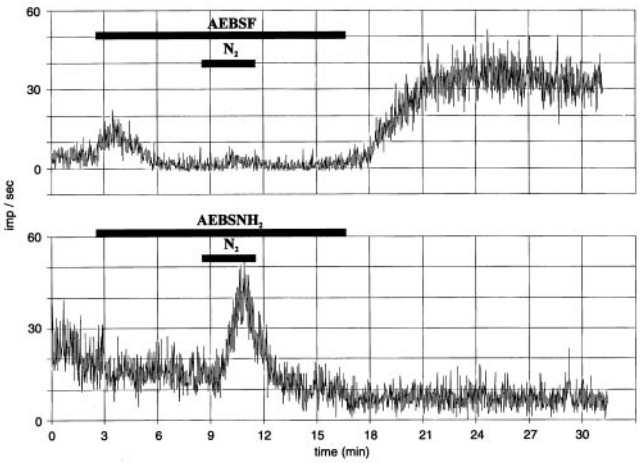

FIG. 4. (*Upper*) AEBSF application to inhibit cytochrome b_{558} (long horizontal bar). After an initial excitation of the chemosensory discharges there is significant inhibition and insensitivity to severe hypoxia induced by N_2 (short horizontal bar, N_2). Washing AEBSF results in marked overshoot of chemoreceptor activity. (*Lower*) The analog AEBSNH2 (long horizontal bar) reduced baseline discharge but did not inhibit the N_2-induced chemoreceptor response (short horizontal bar).

AEBSF. Under AEBSNH2, hypoxia increased the chemoreceptor discharge. During AEBSF superfusion of the carotid body, changes in optical density could not be detected (data not shown).

CO was applied to further characterize the cytochromes participating in carotid body chemoreception. Fig. 5*a* shows that replacing 67.2% N_2 with CO increased the chemoreceptor discharge when the carotid body was under 28.8% O_2. Transilluminating the carotid body tissue for short periods with white light (to record absorption spectra) led to sudden declines of nerve activity. This effect probably was the result of photo dissociation of CO-heme binding involved in the generation of action potentials (4). No significant changes of optical density were seen, confirming the findings of Acker and Xue (6) on negligible redox effects of CO on carotid body cytochromes. Replacing 28.8% O_2 with N_2 stimulated the discharge, and light now increased the discharge rate, which was accompanied by a reduction of the cytochromes.

The redox-dependent photo dissociation of the chemoreceptor discharge was tested in 10 carotid bodies and is summarized in Fig. 5*b*. The chemoreceptor discharge, stimulated by prolonged hypoxia, was used as a reference (marked as 2) in each experiment. The highest discharge level of the peak was 100% at time zero. The CO response curve (marked as 1) was compared with the highest discharge level at time zero in the reference. Photo dissociation (light) of the CO-stimulated chemoreceptor discharge under 28.8% O_2 is shown on the left side of time zero. Light produced an abrupt decline in the chemoreceptor discharge (increased by CO) toward the reference curve. In contrast, photo dissociation under hypoxia resulted in an increased chemoreceptor discharge approaching the reference curve, as shown on the right side of time zero.

The negligible effect of CO on absorption spectra during normoxia, with the simultaneous photolabile effect on nerve activity required another method to identify the heme interacting with CO in the carotid body. For this purpose, five carotid bodies were transilluminated with different wavelengths by using interference filters with a half band width of 10 nm (4). Fig. 6*a* shows that CO increased sinus nerve activity under 28.8% O_2. Transilluminating the carotid body with white light, or with 460–652 nm light of the same intensity, depressed nerve activity to various degrees. The responses to white light (at the beginning and end of the experiment) were used as controls. Fig. 6*b* summarizes the photolabile effects on sinus nerve activity at wavelengths of 543–606 nm. Equalizing the light energy of all points to the level at 460 nm resulted in a peak at 606 nm. Thus, the heme interacting with CO in the rat carotid body (in a redox-dependent manner) seems to have a

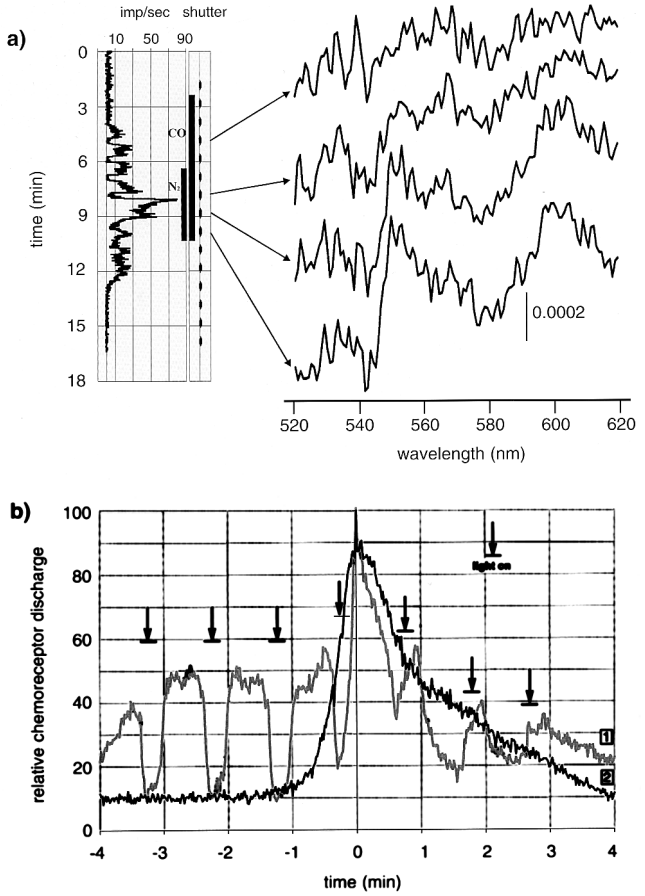

FIG. 5. (*a*) Chemoreceptor discharge (*Left*) and cytochrome redox state (*Right*) under the influence of CO in normoxia leads to discharge increase without light absorption changes (first spectrum trace). Hypoxia (N_2) produces discharge increase with typically reduced cytochrome spectra. Short and repeated transilluminations of carotid body tissue, for recording absorption spectra (small bars in shutter), lead to discharge inhibition during normoxia and excitation during hypoxia. (*b*) Chemoreceptor discharge under normoxic and hypoxic CO applications. (Reference curve 1) Effect of CO as percentage of peak chemoreceptor activity induced by 4-min hypoxia (reference curve 2). Mean of 10 carotid bodies. CO application during normoxia (left side of time zero) lead to excitation, which is eliminated during transient transilluminations (vertical arrows). CO application during hypoxia (right side of time zero) leads to discharge inhibition, which is reversed during transillumination.

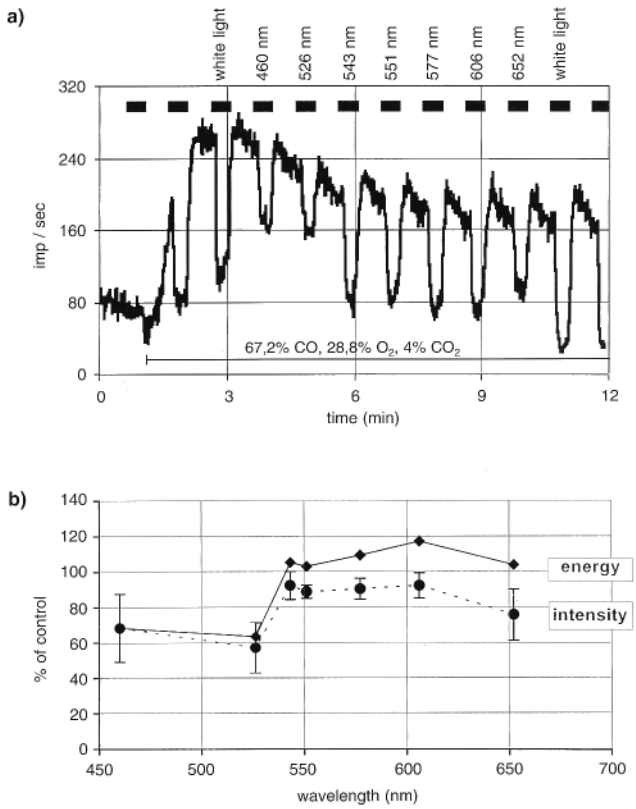

FIG. 6. (*a*) Photolabile reaction of chemoreceptor discharge increase during CO application under normoxia and transilluminations with white light and light of different wavelengths (range 460–652 nm) of the same intensity. CO is applied at the bottom indicated by bar. (*b*) Action spectrum analysis of cytochrome type binding CO in a photolabile manner. Mean of five carotid bodies. One curve shows the photolabile reaction on the basis of equal light intensity at all wavelengths, and the other of same light energy equalized to the level at 460 nm. Wavelengths below 460 nm could not be tested because of the drastically decreased light intensity of the halogen lamp used for transillumination.

broad light absorption spectrum, peaking at about 606 nm, and could be a cytochrome *a*-type heme protein. The photolabile effects of CO were independent of CO_2 stimulation (data not shown).

DISCUSSION

Our experiments showed the relationship between chemoreceptor discharges and the redox state of cytochromes, under the influence of different heme ligands such as oxygen, cyanide, AEBSF, and CO. These agents influence the chemical state of the iron atom of heme proteins (14). All agents induced an initial increase in nerve discharge frequency usually with a logging photometric response. The nerve activity declined during severe hypoxia and cyanide, resulting in a low-discharge steady state, whereas the photometric changes were maintained or declined much more slowly. CO_2 excited the chemoreceptor discharge but this effect was not accompanied by photometric variations.

Concerning the effects of light on chemoreceptor responses, the following is pertinent. CO, when applied to normoxic carotid bodies, excited the chemoreceptors in the dark. Light depressed this response because CO was dissociated from mitochondrial heme. However, during hypoxia, light excited the chemoreceptors, presumably because of reversal of metabolic effects inhibited by CO.

During the second phase (decline in chemoreceptor discharge induced by hypoxia and cyanide), the cytochromes were reduced. Thus, inhibition of chemoreceptor activity was associated with severe reduction of the cytochromes and depressed metabolism. These findings suggest that the redox or metabolic state of chemoreceptor tissues is not the sensor eliciting chemoreceptor discharges. This sensor could be a heme ligand, binding with CO in normoxia, and producing the action potentials (4).

To detect interactions between heme ligands and cytochromes in the rat carotid body by absorption photometry, a nominally hemoglobin-free tissue is a prerequisite. This prerequisite is necessary because the absorption changes of hemoglobin under hypoxia are about 10 times higher (preliminary experiments, data not shown), making all cytochrome absorption peaks undetectable. A second condition is to use spectral analyses of light absorption changes, which allow the identification of single cytochromes by deconvolution. Mitochondrial cytochromes together with cytochrome b_{558} are influenced to different degrees by heme ligands with oxygen and cyanide leading to strong reductions, whereas CO and AEBSF show no detectable changes.

It is important, therefore, to detect possible links between the redox state of cytochromes and chemoreceptor discharges and the identification of the oxygen-sensing proteins. Studies on isolated type I cells have shown that closing of PO_2-dependent potassium channels is linear between 160 and 20 Torr, accompanied by increased intracellular calcium and subsequent transmitter release (16). Also cyanide (up to 1 mM), applied to type I cells, increases intracellular calcium and depresses the mitochondrial membrane potential (3). However, our experiments have shown that the carotid nerve discharge does not follow severe hypoxia or cyanide applications in linear fashion. It declines or disappears after a distinct peak of activity, an effect accompanied by a significant reduction of mitochondrial and nonmitochondrial cytochromes (see Figs. 1 and 2). It seems, therefore, that cytochrome reduction has different influences on the PO_2-sensing properties of type I cells and apposed nerve endings. The silencing of the chemoreceptor discharge when cyanide reduces mitochondrial cytochromes and when AEBSF inhibits the phagocytic cytochrome b_{558} suggest that the functioning of an unimpaired electron carrier in the cytochromes is necessary for a sustained hypoxic response of the carotid nerve. Furthermore, diphenyliodonium (another inhibitor of the phagocytic NADPH oxidase) also inhibits the chemoreceptor discharge after an initial excitation (17).

Mitochondrial cytochromes have been studied for their oxygen-sensing properties in carotid body type I cells (2–4), heart (18), and liver (19). The nonphagocytic, low-output NAD(P)H oxidase has been suggested as the primary oxygen-sensing cytochrome in type I cells (13, 17, 20), neuroepithelial bodies (21), smooth muscle cells of the pulmonary vasculature (22), and hepatoma cells (9). Cytochrome b_{558}, one component of the phagocytic high-output NADPH oxidase, is insensitive to cyanide (17), which we confirmed by deconvolution analyses (see Fig. 2*c*). Several studies have suggested that the nonphagocytic low-output NAD(P)H oxidase, occurring in most cell types, is an isoform of the phagocytic high-output enzyme (23). Differences have been found in the amino acid sequence of gp91phox (24), the polymorphism of the p22phox gene (25), and the involvement of Rac1 or Rac2 in the regulation of the high- and low-output NAD(P)H oxidase (26). These differences may explain how the production of erythropoietin in B cells of chronic granulomatous patients, who suffer from mutations in the phagocytic cytochrome b_{558}, can be induced by hypoxia (27). Also the preserved hypoxic vasoconstriction of lung vessels (in mice lacking the phagocytic gp91phox) suggested a probable function of the low-output NAD(P)H oxidase as an oxygen sensor (28). Figs. 5 and 6 suggest a third candidate, working as an oxygen-sensing cytochrome. CO influences in redox-dependent manner the chemoreceptor discharge. This influence is photolabile, although CO-induced dopamine release from cat carotid body type I cells is not (29). This difference may indicate the capability of carotid body nerve endings to control the generation of action potentials in a PO_2-dependent manner. This property has been studied by Mitchell *et al.* (30) and Kiennecker *et al.* (31) on the PO_2 sensitivity of the nerve discharge of neuromas, formed by regeneration of the carotid sinus nerve. However, Zapata *et al.* (32) observed that crushing the carotid sinus nerve at different distances from the carotid body produced recovery of chemosensory activity only when appositions between nerve fibers and glomus cells were reestablished. These observations do not necessarily exclude their assumed PO_2 sensitivity, but might be the result of a maturation process of the nerve endings under the influence of type I cells to develop oxygen-sensing properties. This process has been observed by Monti-Bloch *et al.* (33), whose findings showed that carotid body grafts induced chemosensitivity in muscle nerve fibers of the cat.

The excitatory effects of CO under normoxia could be caused by binding to a heme, which attached directly to an ion channel, controls its pore size and therewith the membrane potential of nerve endings. Hypoxia has an additional effect on the photolabile CO-heme binding, enhancing inhibition possibly by changing the configuration of the assumed heme, in cooperation with CO. This redox dependency makes it unlikely that the heme identified by Wilson *et al.* (4) as a cytochrome *a* type could be located in mitochondria. This assumption is further substantiated by the prompt light effect on the nerve discharge (probably induced by photo dissociation of the CO-heme binding) bringing back chemoreceptor activity to the normoxic and hypoxic reference curve. The concentration of this heme seems to be low in comparison to cytochromes because no significant change in optical density was observed under normoxic CO applications. We cannot exclude, however, that the prompt photo dissociation of CO-heme binding during transillumination brings back the conformation state to control and eliminates any characteristic absorption peak.

Excitation of chemosensory discharges during normoxia and during moderate hypoxia in the dark by CO and its suppression by light have been reported (34). According to the membrane hypothesis, inhibition of K^+ currents of glomus cell leads to chemosensory excitation. Thus, under normoxia CO should

decrease this K^+ current. But no such observation is available. The only data available are those by Lopez-Lopez and Gonzalez (35) who showed that hypoxic inhibition of K^+ currents is reversed by PO_2 of 70 Torr. This inhibition by CO at a O_2 of 40 Torr is analogous to the high PO_2 effect (36, 37) and apparently is consistent with CO suppression of hypoxic chemosensory excitation (34). However, these authors (35) did not mention whether carotid body glomus cells were exposed to light or darkness, which may have eliminated the mitochondrial effect of CO. Our observations, however, are indications for an ion channel in the nerve ending directly gated by a heme, which already has been hypothesized for type I cells by Lopez-Barneo *et al.* (38). This complex interplay between different mitochondrial and nonmitochondrial cytochromes to establish a chemoreceptor response of the carotid body, in terms of transmitter release and chemoreceptor discharge, makes this organ an ideal model to understand the adaptation of cells to the heterogeneity of tissue PO_2 levels to optimize gene expression and electrical activity (5).

The technical assistance of B. Bülling and E. Merten is gratefully acknowledged. S.L. was awarded a Humboldt Research Award for U.S. Senior Scientists and was a recipient of National Institutes of Health Grants 5R 37 HL-43413 and HL-50180.

1. Gonzalez C., Almaraz, L., Obeso, A. & Rigual, R. (1994) *Physiol. Rev.* **74,** 829–898.
2. Mills, E. & Jōbsis, F. F. (1972) *J. Neurophysiol.* **35,** 405–428.
3. Duchen, M. R. & Biscoe, T. J. (1992) *J. Physiol. (London)* **450,** 13–31.
4. Wilson, D. F., Mokashi, A., Chugh, D., Vinogradov, S., Osanai, S. & Lahiri, S. (1994) *FEBS Lett.* **351,** 370–374.
5. Acker, H. (1994) *Respir. Physiol.* **95,** 1–10.
6. Acker, H. & Xue, D. (1995) *News Physiol. Sci.* **10,** 211–216.
7. Diatchuk, O. L., Koshkin, V., Wikstroem, P. & Pick, E. (1997) *J. Biol. Chem.* **272,** 13292–13301.
8. Delpiano, M. A. & Acker, H. (1989) *Brain Res.* **482,** 235–246.
9. Ehleben, W., Porwol, T., Fandrey, J., Kummer, W. & Acker, H. (1997) *Kidney Int.* **51,** 483–491.
10. Porwol, T., Ehleben, W., Zierold, K., Fandrey, J. & Acker, H. (1998) *Eur. J. Biochem.* **256,** 16–23.
11. Chance, B., Lagallais, V., Sorge, J. & Graham, N. (1975) *Anal. Biochem* **66,** 498–514.
12. Thelen, M., Dewald, B. & Baggiolini, M. (1993) *Physiol. Rev.* **73,** 797–821.
13. Kummer, W. & Acker, H. (1995) *J. Appl. Physiol.* **78,** 1904–1909.
14. Edwards, S. L. & Poulos, T. L. (1990) *J. Biol. Chem.* **265,** 2588–2595.
15. Lahiri, S., Buerk, D. G., Chugh, D., Osanai, S. & Mokashi, A. (1995) *Brain Res.* **684,** 194–200.
16. Montoro, R. J., Ure-a, J., Fernandez-Chacon, R., De Toledo, G. A. & Lopez-Barneo, J. (1996) *J. Gen. Physiol.* **107,** 133–143.
17. Cross, A. R., Henderson, L., Jones, O. T. G., Delpiano, M. A., Hentschel, J. & Acker, H. (1990) *Biochem. J.* **272,** 743–747.
18. Budinger, R. S., Duranteau, J., Chandel, N. S. & Schumacker, P. T. (1998) *J. Biol. Chem.* **273,** 3320–3326.
19. Chandel, N. S., Budinger, G. R. S., Choe, H. & Schumacker, P. T. (1997) *J. Biol. Chem.* **272,** 18808–18816.
20. Youngson, C., Nurse, C., Yeger, H., Curnutte, J. T., Vollmer, C., Wong, V. & Cutz, E. (1997) *Microsc. Res. Tech.* **37,** 101–106.
21. Wang, D. S., Youngson, C., Wong, V., Yeger, H., Dinauer, M. C., Derniera, E. V. S., Rudy, B. & Cutz, E. (1996) *Proc. Natl. Acad. Sci. USA* **93,** 13182–13187.
22. Marshall, C., Mamary, A. J., Verhoeven, A. J. & Marshall, B. E. (1996) *Am. J. Respir. Cell Mol. Biol.* **15,** 633–644.
23. Bastian, N. R. & Hibbs, J. B., Jr. (1994) *Curr. Opin. Immunol.* **6,** 131–139.
24. Moulton, P., Goldring, M. B. & Hancock, J. T. (1998) *Biochem. J.* **329,** 449–451.
25. Inoue, N., Kawashima, S., Kanawaza, K., Yamada, S., Akita, S. & Yokoyama, M. (1998) *Circulation* **97,** 135–137.
26. Cool, R. H., Merten, E., Theiss, Ch. & Acker, H. (1998) *Biochem. J.* **332,** 5–8.
27. Wenger, R. H., Marti, H. H., Schuerer-Maly, C. C., Kvietikova, I., Bauer, C., Gassmann, M. & Maly, F. E. (1996) *Blood* **87,** 756–761.
28. Archer, S. L., Reeve, H. L., Nelson, D. P., Dinauer, M. C. & Weir, E. K. (1999) *Proc. Natl. Acad. Sci. USA*, in press.
29. Buerk, D. G., Chugh, D. K., Osanai, S., Mokashi, A. & Lahiri, S. (1997) *J. Auton. Nerv. Syst.* **67,** 130–136.
30. Mitchell, R. A., Sinha, A. K. & McDonald, D. M. (1972) *Brain Res.* **43,** 1077–1088.
31. Kiennecker, E. W., Knoche, H. & Bingmann, D. (1978) *Neuroscience* **3,** 977–988.
32. Zapata, P., Stensaas, J. & Eyzaguirre, C. (1976) *Brain Res.* **113,** 235–253.
33. Monti-Bloch, L., Stensaas, L. J. & Eyzaguirre, C. (1983) *Brain Res.* **270,** 77–92.
34. Lahiri, S., Iturriaga, R., Mokashi, A., Ray, D. K. & Chugh, D. (1993) *Respir. Physiol.* **75,** 227–240.
35. Lopez-Lopez, J. R. & Gonzalez, C. (1992) *FEBS Lett.* **299,** 251–254.
36. Lloyd, B. B., Cunningham, D. J. C. & Goode, R. C. (1968) in *Arterial Chemoreceptors*, ed. Torrance, R. W. (Blackwell, Oxford), pp. 144–148.
37. Huang, L. E., Willmore, W., Gu, J., Goldberg, M. A. & Bunn, H. F. (1999) *J. Biol. Chem.* **274,** 9038–9044.
38. Lopez-Barneo, J., Benot, A. R. & Ureña, J. (1993) *News Physiol. Sci*. **8,** 191–195.